

Measuring the speed of sound of the quark-gluon plasma in ultracentral nucleus-nucleus collisions

Fernando G. Gardim,^{1,2} Giuliano Giacalone,² and Jean-Yves Ollitrault²

¹*Instituto de Ciência e Tecnologia, Universidade Federal de Alfenas, 37715-400 Poços de Caldas, MG, Brazil*

²*Institut de physique théorique, Université Paris Saclay, CNRS, CEA, F-91191 Gif-sur-Yvette, France*

We show that, within the hydrodynamic framework of heavy-ion collisions, the mean transverse momentum of charged hadrons ($\langle p_t \rangle$) rises as a function of the multiplicity in ultra-central nucleus-nucleus collisions. The relative increase is proportional to the speed of sound squared (c_s^2) of the quark-gluon plasma, that is therefore accessible experimentally using ultra-central data. Based on the value of c_s^2 calculated in lattice QCD, we predict that $\langle p_t \rangle$ increases by ~ 18 MeV between 1% and 0.001% centrality in Pb+Pb collisions at $\sqrt{s_{\text{NN}}} = 5.02$ TeV.

Introduction. We propose a method to determine experimentally the speed of sound of the quark-gluon plasma produced in ultrarelativistic heavy-ion collisions. The speed of sound, c_s , is the velocity at which a compression wave travels in a fluid. Its magnitude is determined by the change in pressure as one increases the density. In a relativistic fluid, it is given by [1]

$$c_s^2 = \frac{dP}{d\epsilon} = \frac{d \ln T}{d \ln s}, \quad (1)$$

where P , ϵ , T , s denote the pressure, energy density, temperature, and entropy density.

The idea is that ultra-central collisions (defined for instance as the 0.1% most central collisions) produce a quark-gluon plasma which always has the same volume, while the particle multiplicity N_{ch} can vary by a few percent (typically 5% to 10%, depending on the experiment). The entropy is proportional to the multiplicity, and the volume is constant, therefore, the entropy *density* s is itself proportional to the multiplicity, and also varies by a few percent. As a consequence, the temperature increases as a function of the multiplicity, and this implies a rise of the mean transverse momentum of charged hadrons [2], which can be measured.

Recent analyses [3] seem to contradict this prediction: $\langle p_t \rangle$ varies by less than 0.2% in the 0-20% centrality range in Pb+Pb collisions at $\sqrt{s_{\text{NN}}} = 5.02$ TeV. However, these analyses use wide centrality bins, while the rise is only expected in ultra-central collisions. The observed flatness of $\langle p_T \rangle$ implies that even a modest rise in the ultra-central range [4–6] will be easy to identify. This rise allows to determine the speed of sound directly as a function of experimental quantities using

$$c_s^2 = \frac{d \ln \langle p_t \rangle}{d \ln N_{\text{ch}}}. \quad (2)$$

This analysis requires to bin events in N_{ch} or, equivalently, to determine the centrality using N_{ch} [6]. We use N_{ch} as a measure of the entropy and $\langle p_t \rangle$ as a measure of the temperature. Consistency then requires that both should be measured in the same rapidity window, at variance with current analyses where centrality is typically determined in a separate rapidity window [7].

We now carry out a quantitative analysis using an effective hydrodynamic description [2] and a realistic model of initial conditions [8]. We then propose a refinement of Eq. (2) that allows to determine the speed of sound experimentally using information inferred from the distribution of N_{ch} .

Effective hydrodynamic description. The speed of sound of the quark-gluon plasma is not a constant, it depends on its temperature. Now, the quark-gluon plasma produced in a heavy-ion collision is inhomogeneous, and cools rapidly by expanding into the vacuum, so that its temperature depends on space-time coordinates. In order to average out this dependence, we define an effective temperature T_{eff} and an effective volume V_{eff} , which are those of a uniform fluid at rest which would have the same energy, E , and entropy, S , as the fluid at the end of the hydrodynamic evolution (freeze-out). Detailed ideal hydrodynamic calculations [2] show that:

$$\begin{aligned} T_{\text{eff}} &= \frac{1}{3.07} \langle p_t \rangle \\ V_{\text{eff}} &= 1.2\pi R^3, \end{aligned} \quad (3)$$

where R is the transverse radius of the system at the beginning of the hydrodynamic evolution. This radius is defined by

$$R^2 \equiv 2 (\langle \mathbf{r}^2 \rangle - \langle \mathbf{r} \rangle^2), \quad (4)$$

where $\mathbf{r} = (x, y)$ is the transverse coordinate, and angular brackets denote an average value taken with the initial entropy density as a weight.¹ Inclusion of shear and bulk viscosity changes slightly the proportionality coefficient between V_{eff} and R^3 , not between $\langle p_t \rangle$ and T_{eff} .

Equations (3) imply that:

- The mean transverse momentum of charged hadrons is directly proportional to T_{eff} . Therefore, the value of c_s inferred from the variation of $\langle p_t \rangle$ as a function of the multiplicity is equal to the speed of sound evaluated at T_{eff} , whose value is $T_{\text{eff}} = 222 \pm 9$ MeV in central Pb+Pb collisions at $\sqrt{s_{\text{NN}}} = 5.02$ TeV [2].

¹ The factor 2 ensures that the right-hand side is equal to R^2 if the entropy density is uniform in a circle of radius R .

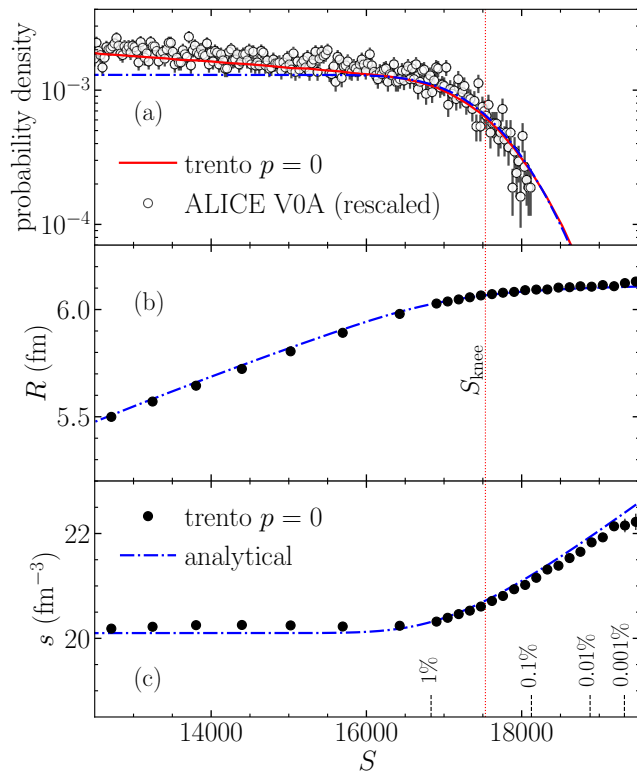


FIG. 1. Results from the TRENTo model of initial conditions [8], with $p = 0$ and $k = 2.0$. 20 million Pb+Pb collisions at $\sqrt{s_{NN}} = 5.02$ TeV were generated. Only 10% of these events, corresponding to the largest values of the total entropy per unit rapidity S (0-10% centrality), are used. (a) Full line: Probability distribution of S in the TRENTo calculation. Open symbols: Probability distribution of the V0 amplitude, used by ALICE to determine the centrality [9], rescaled by a factor 0.51. (b) Initial radius R (Eq. (4)). (c) Effective entropy density s (Eq. (5)). Symbols in panels (b) and (c) are results from the TRENTo simulation, averaged over events. Dot-dashed lines in panels (a), (b) and (c) are one parameter fits using Eqs. (9), (12) and (13). Vertical lines spot specific values of the centrality percentile, and the position of the knee.

- The entropy density at T_{eff} is given by

$$s(T_{\text{eff}}) = \frac{S}{V_{\text{eff}}} = \frac{S}{1.2\pi R^3}, \quad (5)$$

which is simply denoted by s below. It can be determined from the initial conditions of the hydrodynamic calculation, since hydrodynamics conserves entropy to a good approximation.

Quantitative analysis. We now show explicitly, using a realistic model of initial conditions, that the effective entropy density is proportional to the multiplicity in ultra-central collisions. We use the TRENTo Monte Carlo generator of initial conditions [8] with the $p = 0$ prescription (corresponding to an entropy density proportional

to $\sqrt{T_A T_B}$, where T_A and T_B are the thickness functions of incoming nuclei [10]), which gives good agreement with data [11]. We tune the fluctuation parameter of TRENTo, k , in such a way that the distribution of entropy (we denote by S the total entropy per unit rapidity) coincides, up to a global multiplicative constant, with the distribution of the multiplicity (V0 amplitude) used by ALICE to define the centrality of Pb+Pb collisions at $\sqrt{s_{NN}} = 5.02$ TeV [9]. The same choice of parameters also reproduces the distribution of N_{ch} measured by ATLAS [6]. In addition, we have multiplied the entropy given by the TRENTo model by a constant coefficient so that the entropy density in central collisions matches the value $s \sim 20 \text{ fm}^{-3}$ extracted from a recent analysis of Pb+Pb data [2].

The distribution of S is displayed in Fig. 1 (a). Two different regimes can be observed left and right of the *knee*, to be defined below (Eq. (7)). Left of the knee, the distribution decreases slowly. The variation of S in this region is driven by the variation of impact parameter. Right of the knee, the distribution decreases steeply. In this region, the variation of S is driven by initial-state fluctuations.

Figure 1 (b) displays the value of the initial radius R (Eq. (4)), averaged over events, as a function of S . It increases and then saturates around the value of the knee, confirming the intuitive idea that events beyond the knee share the same geometry.

Figure 1 (c) displays the effective entropy density s , defined by Eq. (5), averaged over events. Left of the knee, this effective density is essentially constant, which in turn implies that the effective temperature T_{eff} and the mean transverse momentum $\langle p_t \rangle$ are also constant, in agreement with experimental data (see below Fig. 2). The essential point of this paper is that right of the knee, the entropy density starts rising because the volume becomes constant, so that s is proportional to S .

Analytic model. We now derive a simple parametrization which captures the trends observed in Fig. 1. We first assume that the probability distribution of S at a fixed impact parameter b is a Gaussian [13]:

$$P(S|b) = \frac{1}{\sigma\sqrt{2\pi}} \exp\left(-\frac{(S - \bar{S}(b))^2}{2\sigma^2}\right), \quad (6)$$

where $\bar{S}(b)$ is the mean value, which decreases with increasing b , and σ is the width, whose dependence on b is neglected. The knee is defined as the mean value of S at $b = 0$:

$$S_{\text{knee}} \equiv \bar{S}(0). \quad (7)$$

We first derive the distribution of S by integrating over impact parameter. We change variables $b \rightarrow \bar{S}(b)$, so that Eq. (6) becomes

$$P(S|\bar{S}) = \frac{1}{\sigma\sqrt{2\pi}} \exp\left(-\frac{(S - \bar{S})^2}{2\sigma^2}\right). \quad (8)$$

We then integrate over \bar{S} :

$$\begin{aligned} P(S) &= \int_0^{S_{\text{knee}}} P(S|\bar{S})P(\bar{S})d\bar{S} \\ &\propto \int_0^{S_{\text{knee}}} P(S|\bar{S})d\bar{S} \\ &\propto \text{erfc}\left(\frac{S - S_{\text{knee}}}{\sigma\sqrt{2}}\right), \end{aligned} \quad (9)$$

where we have assumed for simplicity that the probability distribution of \bar{S} , $P(\bar{S})$, is constant. This model is displayed as a dashed line in Fig. 1 (a). The parameters S_{knee} and σ have been obtained within the TRENTO model by computing the mean and standard deviation of the distribution of S at $b = 0$. The proportionality constant is adjusted by hand. This simple model captures the trends observed in the TRENTO simulation up to 10% centrality.

Next, we assume that the initial radius R only depends on impact parameter, or equivalently, on \bar{S} . In order to determine R for fixed S , we first determine the distribution of \bar{S} for fixed S using Bayes' theorem:

$$P(\bar{S}|S) = \frac{P(S|\bar{S})P(\bar{S})}{P(S)}. \quad (10)$$

The average value of \bar{S} for fixed S is obtained by inserting Eq. (8) into Eq. (10) and integrating over \bar{S} . Assuming again that $P(\bar{S})$ is approximately constant, we obtain:

$$\langle \bar{S}|S \rangle = S - \sigma \sqrt{\frac{2}{\pi}} \frac{\exp\left(-\frac{(S-S_{\text{knee}})^2}{2\sigma^2}\right)}{\text{erfc}\left(\frac{S-S_{\text{knee}}}{\sqrt{2}\sigma}\right)}. \quad (11)$$

For $S < S_{\text{knee}}$, the second term in the right-hand side is negligible and $\langle \bar{S}|S \rangle \simeq S$, i.e., fluctuations are averaged out [14]. Right of the knee, \bar{S} saturates to its maximum value: $\langle \bar{S}|S \rangle \simeq S_{\text{knee}}$.

The observation that the entropy density is constant left of the knee in the TRENTO calculation suggests that the volume is proportional to \bar{S} . Under this assumption, the radius R is given by

$$R = R_0 \left(\frac{\langle \bar{S}|S \rangle}{S_{\text{knee}}}\right)^{1/3} \quad (12)$$

while the entropy density is given by

$$s = s_0 \frac{S}{\langle \bar{S}|S \rangle}. \quad (13)$$

In these equations, R_0 and s_0 are fit parameters which correspond to the value of R right of the knee, and the value of s left of the knee, respectively. Panels (b) and (c) of Fig. 1 show that Eqs. (12) and (13) give good fits of the full TRENTO simulation.

Quantitative predictions for Pb+Pb collisions at $\sqrt{s_{\text{NN}}} = 5.02$ TeV. We now make quantitative predictions using this simple parametrization, which we consider to be more general than the particular model of initial conditions for which we have tested it. The interest is

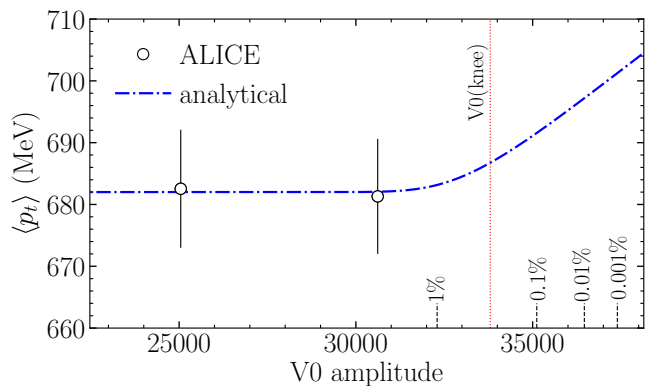


FIG. 2. Line: our prediction for the variation of $\langle p_t \rangle$ with the V0 amplitude in Pb+Pb collisions at $\sqrt{s_{\text{NN}}} = 5.02$ TeV. Symbols are data from the ALICE collaboration [3].

that the parameters can be determined from data. More specifically, one replaces S with the charged-particle multiplicity N_{ch} . The quantities S_{knee} and σ can then be determined from the distribution of N_{ch} . This can be done either using the simple Bayesian procedure of Ref. [13], or by fitting a model (such as the Glauber model) to the experimental histogram and computing S_{knee} and σ in the model. We apply the procedure of Ref. [13] to ALICE data, using the V0 amplitude as a proxy for the charged multiplicity [7] and using the data shown in Fig. 1 (a). We next assume that the mean transverse momentum is proportional to the temperature, which is itself proportional to s^c_s if one neglects the variation of c_s^2 in Eq. (1). Using Eq. (13), we obtain the prediction:

$$\langle p_t \rangle = p_{t0} \left(\frac{S}{\langle \bar{S}|S \rangle}\right)^{c_s^2}, \quad (14)$$

where p_{t0} is the value of $\langle p_t \rangle$ left of the knee, and $\langle \bar{S}|S \rangle$ is given by Eq. (11). We use the value $p_{t0} = 682$ MeV measured by ALICE in the 0-5% centrality range [3]. As anticipated, this value corresponds to an effective temperature $T_{\text{eff}} = 222$ MeV according to Eq. (3), at which lattice QCD predicts $c_s^2 = 0.252$ [15]. This yields the prediction displayed in Fig. 2. We predict that $\langle p_t \rangle$ increases by 8.4 MeV between 1% and 0.1% centrality, by 5.6 MeV between 0.1% and 0.01%, and by 4.1 MeV between 0.01% and 0.001%. These predictions are however approximate for two reasons. First, we are using the multiplicity inferred from the V0 amplitude, which is measured in a different rapidity window than $\langle p_t \rangle$. Second, the observed multiplicity fluctuation gets a small contribution from trivial statistical (Poisson) fluctuations, which do not contribute to the rise of $\langle p_t \rangle$. In the case of ATLAS data [6] on the distribution of N_{ch} , the width of Poisson fluctuations is smaller by a factor 2.5 than the total width. Assuming that statistical and dynamical fluctuations add up in quadrature, this implies that the width of dynamical fluctuations is 90% of the total

width. Thus one expects a 10% reduction of the rise of $\langle p_t \rangle$ due to trivial statistical fluctuations.

Equation (14) coincides with Eq. (2) for the most central events, where $\langle \bar{S} | S \rangle$ saturates. Its advantage over Eq. (2) is that it can be used all the way up to 10% centrality. Experimentally, c_s can be measured by fitting Eq. (14) to data, using p_{t0} and c_s as fit parameters. Such an analysis would complement the extraction of c_s from the variation of $\langle p_t \rangle$ with $\sqrt{s_{NN}}$ [2]. More importantly, the predicted rise of $\langle p_t \rangle$ in ultra-central collisions is a non-trivial test of hydrodynamic behavior which does

not involve anisotropic flow [16].

ACKNOWLEDGMENTS

F.G.G. was supported by Conselho Nacional de Desenvolvimento Científico e Tecnológico (CNPq grant 205369/2018-9 and 312932/2018-9). F.G.G. acknowledges support from project INCT-FNA Proc. No. 464898/2014-5.

-
- [1] J. Y. Ollitrault, Eur. J. Phys. **29**, 275 (2008) doi:10.1088/0143-0807/29/2/010 [arXiv:0708.2433 [nucl-th]].
- [2] F. G. Gardim, G. Giacalone, M. Luzum and J. Y. Ollitrault, arXiv:1908.09728 [nucl-th].
- [3] S. Acharya *et al.* [ALICE Collaboration], Phys. Lett. B **788**, 166 (2019) doi:10.1016/j.physletb.2018.10.052 [arXiv:1805.04399 [nucl-ex]].
- [4] M. Luzum and J. Y. Ollitrault, Nucl. Phys. A **904-905**, 377c (2013) doi:10.1016/j.nuclphysa.2013.02.028 [arXiv:1210.6010 [nucl-th]].
- [5] S. Chatrchyan *et al.* [CMS Collaboration], JHEP **1402**, 088 (2014) doi:10.1007/JHEP02(2014)088 [arXiv:1312.1845 [nucl-ex]].
- [6] M. Aaboud *et al.* [ATLAS Collaboration], [arXiv:1904.04808 [nucl-ex]].
- [7] B. Abelev *et al.* [ALICE Collaboration], Phys. Rev. C **88**, no. 4, 044909 (2013) doi:10.1103/PhysRevC.88.044909 [arXiv:1301.4361 [nucl-ex]].
- [8] J. S. Moreland, J. E. Bernhard and S. A. Bass, Phys. Rev. C **92**, no. 1, 011901 (2015) doi:10.1103/PhysRevC.92.011901 [arXiv:1412.4708 [nucl-th]].
- [9] J. Adam *et al.* [ALICE Collaboration], Phys. Rev. Lett. **116**, no. 22, 222302 (2016) doi:10.1103/PhysRevLett.116.222302 [arXiv:1512.06104 [nucl-ex]].
- [10] M. L. Miller, K. Reygers, S. J. Sanders and P. Steinberg, Ann. Rev. Nucl. Part. Sci. **57**, 205 (2007) doi:10.1146/annurev.nucl.57.090506.123020 [nucl-ex/0701025].
- [11] G. Giacalone, J. Noronha-Hostler, M. Luzum and J. Y. Ollitrault, Phys. Rev. C **97**, no. 3, 034904 (2018) doi:10.1103/PhysRevC.97.034904 [arXiv:1711.08499 [nucl-th]].
- [12] S. Acharya *et al.* [ALICE Collaboration], JHEP **1811**, 013 (2018) doi:10.1007/JHEP11(2018)013 [arXiv:1802.09145 [nucl-ex]].
- [13] S. J. Das, G. Giacalone, P. A. Monard and J. Y. Ollitrault, Phys. Rev. C **97**, no. 1, 014905 (2018) doi:10.1103/PhysRevC.97.014905 [arXiv:1708.00081 [nucl-th]].
- [14] W. Broniowski and W. Florkowski, Phys. Rev. C **65**, 024905 (2002) doi:10.1103/PhysRevC.65.024905 [nucl-th/0110020].
- [15] S. Borsanyi, Z. Fodor, C. Hoelbling, S. D. Katz, S. Krieg and K. K. Szabo, Phys. Lett. B **730**, 99 (2014) doi:10.1016/j.physletb.2014.01.007 [arXiv:1309.5258 [hep-lat]].
- [16] U. Heinz and R. Snellings, Ann. Rev. Nucl. Part. Sci. **63**, 123 (2013) doi:10.1146/annurev-nucl-102212-170540 [arXiv:1301.2826 [nucl-th]].